10440
NACA TN 4106

TECH LIBRARY KAFB, NM
0066976

NATIONAL ADVISORY COMMITTEE FOR AERONAUTICS

TECHNICAL NOTE 4106

IMPACT-LOADS INVESTIGATION OF A CHINE-IMMERSED MODEL HAVING A LONGITUDINALLY CURVED BOW AND A V-BOTTOM WITH A DEAD-RISE ANGLE OF 30°

By Philip M. Edge, Jr., and John S. Mixson

Langley Aeronautical Laboratory
Langley Field, Va.

Washington
September 1957

AFMDC
TECHNICAL LIBRARY
AFL 2811

TECH LIBRARY KAFB, NM

0066976

1D

NATIONAL ADVISORY COMMITTEE FOR AERONAUTICS

TECHNICAL NOTE 4106

IMPACT-LOADS INVESTIGATION OF A CHINE-IMMERSED MODEL HAVING A LONGITUDINALLY CURVED BOW AND A V-BOTTOM WITH A DEAD-RISE ANGLE OF 30°

By Philip M. Edge, Jr., and John S. Mixson

SUMMARY

As part of a program to study the effects of transverse and longitudinal curvature on impact loads of chine-immersed models, a V-bottom model having a dead-rise angle of 30° and the forward half longitudinally curved upward on a radius of 10 beams has been tested at the Langley impact basin. Impacts were made in smooth water at a beam-loading coefficient of 18.8 with the trim angle held fixed throughout each impact. Impacts with forward speed were made over a range of trim angles from -3° to 30° and initial flight-path angles from 3.5° to 27°, and a few impacts without forward speed were made at a trim angle of 0° for several vertical velocities.

The data are presented and analyzed to determine the extent of bow immersion during the impacts. The curved bow was found to be not immersed at the high trim angles (15° and 30°), only slightly immersed at trim angles of 6° and 9°, and almost totally immersed at trim angles of 3° and below. The impact loads and motions obtained are presented in coefficient form as variations with trim and initial flight-path angles. The maximum impact loads are shown to be in substantial agreement with loads predicted by theory for the non-bow-immersed case; however, comparisons at 3° trim, where the bow is immersed, show maximum loads that are less than the loads predicted by theory for a straight-keel model.

INTRODUCTION

At the Langley impact basin a program has been underway to determine the relations of model configuration to hydrodynamic impact loads of chine-immersed bodies. This program has dealt primarily with transverse shapes, the effects of longitudinal shape having been included only in tests of a single concave-convex transverse shape (reported in ref. 1). The investigation reported herein was concerned with impact loads experienced by a V-bottom model having a dead-rise angle of 30° and a longitudinally curved bow of approximately half the model length. The bow of

the model was curved upward on a radius of 10 beams and the model had a length-beam ratio of approximately 10. This investigation consisted of a series of impacts at fixed trim in smooth water at a beam-loading coefficient of 18.8 and over a range of flight-path angles at each of several trim angles. The impact conditions ranged from the case where only the straight portion is immersed, through a transition case where small amounts of bow curvature are immersed, to the case of almost total immersion of the curved bow.

This paper presents the impact-loads data obtained from this investigation and discusses the extent of curved-bow immersion and its effect on loads and motions during the impact process. The loads data are expressed in coefficient form to show generalized variations with trim and initial flight-path angles. Also included are comparisons of the maximum loads obtained with the curved-bow model and loads predicted by theory for a straight-keel model. Finally, several general observations are made as to the effect of longitudinal curvature from the standpoint of impact loads on chine-immersed models of this configuration.

SYMBOLS

b	model beam, ft
F_v	vertical component of resultant hydrodynamic force normal to undisturbed water surface, lb
g	acceleration due to gravity, 32.2 ft/sec^2
l_w	wetted model length measured from step-keel point, ft
M_Y	pitching moment about the step-keel point, lb-ft
n_i	impact load factor normal to undisturbed water surface, F_v/W
t	time after water contact, sec
V	resultant velocity, ft/sec
W	dropping weight, lb
$\dot{x}$	velocity of model parallel to undisturbed water surface, ft/sec
z	draft of lowest point of model normal to undisturbed water surface, ft

$\dot{z}$ velocity of model normal to undisturbed water surface, ft/sec

γ flight-path angle, relative to undisturbed water surface, deg

ρ mass density of water, 1.938 slugs/cu ft

τ trim angle (angle between straight keel and undisturbed water surface), deg

C_L impact lift coefficient, $\frac{F_v}{\frac{1}{2}\rho V_o^2 b^2}$

C_d draft coefficient, z/b

C_t time coefficient, $\frac{V_o t}{b}$

C_V vertical-velocity coefficient, $\dot{z}/\dot{z}_o$

C_m pitching-moment coefficient, $\frac{M_Y}{\frac{1}{2}\rho V_o^2 b^3}$

C_{cp} center-of-pressure coefficient, $\frac{\text{Center of pressure measured from step-keel point}}{b}$

C_Δ beam-loading coefficient, $\frac{W}{\rho g b^3}$

Subscripts:

o instant of initial contact with water surface

max maximum

APPARATUS AND TEST PROCEDURE

The tests were made in the Langley impact basin which is described in reference 2 along with its basic instrumentation.

Model

The model tested was about 11 feet long with a beam of 1 foot. The rear half of the bottom had a straight keel and the forward half

was curved upward on a 10-foot radius. The plan form of the step was rectangular and the plan form of the nose was arbitrarily curved. The model was of sheet-metal construction with the V-bottom of wood covered with fiber glass. The bottom was constructed so that a transverse section taken perpendicular to the keel at any point had a dead-rise angle of 30°. Detail lines of the model are shown in figure 1, and a photograph of the model mounted on the carriage boom is shown in figure 2.

Instrumentation

The instruments consisted of an accelerometer, a dynamometer, a water-contact indicator, and electrical pickups for measuring displacements and velocities. The data from these instruments were recorded on a multichannel oscillograph along with 0.01-second timing.

Accelerations were measured in the vertical direction by an unbonded strain-gage-type accelerometer having a range of ±6g and a natural frequency of 17 cycles per second. Pitching moments about the step M_Y were obtained from a strain-gage-type dynamometer mounted between the model and the carriage boom. These moments about the step consisted of the recorded moments (measured about the front attachment point, fig. 2, and transferred to the step) plus the moments due to the acceleration of the mass below the dynamometer (as calculated from the weight and center of gravity of the lower mass and the model acceleration).

Model contact with the water was indicated by means of an electric circuit completed by the water. Horizontal and vertical displacements were obtained from a photoelectric cell and slide-wire, respectively, as described in reference 2. Vertical velocity of the model was determined by means of a generator driven by the vertical movement of the boom.

In general, the apparatus used in this test yields measurements that are believed correct within the following limits:

Horizontal velocity, ft/sec	±0.5
Vertical velocity, ft/sec	±0.2
Vertical displacement, in.	±0.2
Acceleration, g units	±0.2
Weight, lb	±10
Time, sec	±0.002

Test Procedure

A series of impacts were made at fixed trim in smooth water at a beam-loading coefficient C_Δ of 18.8 (dropping weight = 1,170 pounds). The impacts were made over a range of trims, velocities, and flight-path

angles, the directions of which are indicated in figure 1. Impacts with forward speed were made at trim angles of -3°, 0°, 3°, 6°, 9°, 15°, and 30° and initial flight-path angles ranging from 3.5° to 27° (velocity range: $\dot{z}_o$ = 5.4 to 12.4 ft/sec, $\dot{x}_o$ = 22.5 to 89.3 ft/sec). Impacts without forward speed (γ_o = 90°) were made at 0° trim and at several vertical velocities. During each impact a force equal in magnitude and opposite in direction to the total weight of the model and drop linkage was applied to simulate wing lift (ref. 2).

RESULTS AND DISCUSSION

The data obtained for each impact in the investigation are presented in table I along with values of load and pitching moment in coefficient form. Since the rear half of the model is longitudinally straight and the forward half is longitudinally curved, analysis of these data is first concerned with evaluating the impacts as to the amount of bow curvature immersed during the impact processes. Once the shape of the portion of the model involved is understood, the variations of the loads and moment coefficients with trim and flight-path angles can be analyzed for indications of bow effects, and comparisons can be made with loads predicted by theory (ref. 3) for models without longitudinal curvature.

Extent of Bow Immersion During Impact

The extent of bow immersion during the impacts was determined from the shape and trim angle of the model together with the draft of the model. This method of determining bow immersion is based on the intersection of the level water with the model and neglects the effect of water pileup. (Ref. 4 presents pressure distributions which indicate water pileup to be small for this dead-rise angle at similar impact conditions.) The drafts at which the curved bow becomes immersed at the keel and at the chine of the model are presented in table II for each trim angle. By comparing these geometric values of draft at bow immersion with the draft measurements of table I, the time at which the bow becomes involved during each impact can be roughly established. From these tabulated values it is seen that bow immersion for these impacts is limited to the impacts at trim angles below 30°, and that, at 15° trim angle, bow immersion occurs only after maximum load and at high flight-path angles.

In order to indicate the immersion of parts of the bow prior to maximum load for impacts at each of the trim angles, the variation of draft coefficient at maximum load with initial flight-path angle is shown in figure 3 along with geometric values of draft at bow immersion for each trim. This figure, which shows the draft in coefficient form C_d, consists of the geometric values at which the bow becomes immersed at each

trim (represented by two horizontal lines) and of the experimental values for draft at $n_{i,max}$ (represented by symbols). Because the curved bow at the keel is involved at water contact $(C_d = 0)$ for $\tau = 0^\circ$ and -3°, only the draft corresponding to bow immersion of the chines appears in the figure. From this figure several observations are made of the extent of bow immersion at maximum load:

Trim, τ, deg	γ_o, deg	Bow immersion at maximum load
-3	All values	Curved keel and curved chine immersed
0 and 3	<5	Curved keel immersed
0 and 3	>5	Curved keel and curved chine immersed
6	All values	Curved keel immersed
9	>10	Curved keel immersed
15 and 30	All values	None

Figure 3, therefore, indicates that the curved bow of the model becomes involved in the impact process prior to maximum load at trims of 9° and below. At this bow immersion the effect of the curved bow on the maximum impact load is probably dependent upon the shape of the bottom surface which is immersed prior to maximum load. The maximum bottom surface (excluding water rise) involved for each trim at maximum load is illustrated in figure 4. From this figure it can be seen that the curved area involved at maximum load is large, as compared with the straight area involved, only at -3° trim. At 0° and 3° trim the curved area involved at maximum load is shown to be less than one-half the straight area involved. At 6° and 9° trim the maximum curved areas involved are nearly the same and are small when compared with the straight portion involved.

From the results shown in figures 3 and 4 the curved bow of this model configuration is indicated to be of significance during the impact process only at low angles of trim (3° and less). As might be expected, the data obtained at higher trims are indicated to be the same as would be obtained from a similar model without bow curvature as the bow was not immersed or only slightly immersed at maximum impact load for the landing conditions experienced.

Variation of Loads and Motions With Trim and Flight-Path Angle

The vertical load, center-of-pressure, pitching-moment, draft, vertical-velocity, and time coefficients are shown varying with initial flight-path angle for each of the trim angles (figs. 5 to 12). The

variations of the coefficients at the lower trims where the curved bow is involved and the variations for the higher trim angles are compared for indications of effects of bow curvature.

In figure 5 the experimental maximum loads are compared with the loads predicted by theory (ref. 3) for impacts of a similar model without longitudinal curvature. Loads predicted by theory in this manner are limited to positive trims where the impact involves prismatic shapes only. Substantial agreement is indicated at trims of 6° and above between experimental loads obtained with the curved-bow model and loads predicted by theory for a straight-keel model. At 3° trim angle, which is the only trim involving appreciable bow immersion for which comparisons with theory are made, the experimental loads are somewhat less than the loads predicted by theory for a straight-keel model. Since the experimental data indicate that the theory apparently underestimates loads in the high trim range, the theory might overestimate these loads in this low trim range.

Figure 6 shows the variation of maximum load with initial flight-path angle as predicted by theory (fig. 6(a)) for a straight-bow model and as obtained from experiment with the curved-bow model (fig. 6(b)) for all of the trims tested. Comparison of the variations shown indicates that the maximum loads obtained with the curved-bow model vary in a similar manner to those predicted by theory for the straight model; however, there is a greater spread with trim indicated by theory for the straight model. Apparently trim angle is of less importance to the maximum loads of a model of this bow curvature than would be theoretically expected for a straight-keel model.

The variation of center of pressure at maximum impact load with initial flight-path angle is shown in figure 7 in coefficient form and in figure 8 as the ratio of center of pressure to wetted length. From figure 7 it is seen that at the low angles of trim where the bow is involved the center of pressure is well forward at the low initial flight-path angles. Figure 8 shows that, where negligible amounts of bow curvature are involved ($\tau = 6^{\circ}$ and above), the center of pressure scatters about a point at 0.5 of the wetted length. However, at conditions of substantial bow immersion ($\tau = 3^{\circ}$ and below) the center of pressure is in general greater than 0.6 of the wetted length.

The variations of pitching-moment coefficient at maximum load with initial flight-path angle are shown in figure 9. The general trends of increasing pitching moment with increased flight-path angle apparently become more pronounced at the low trim angles where the bow is immersed ($\tau = 3^{\circ}$ and lower).

The variations of maximum draft and draft at maximum load with initial flight-path angle are shown in figure 10. Maximum draft (fig. 10(a)) is shown to be largely independent of trim angle, whereas

the draft at maximum load (fig. 10(b)) generally increases with trim angle for the positive trims. The trend of the draft at maximum load for -3° trim might be explained as in reference 5 by the presence of a reduced-pressure area on part of the bottom at low initial flight-path angles. This reduced-pressure area, caused by the flow pattern set up by initial contact of the water with the curved bow, reduces the vertical force, which then requires greater time and draft in order to build up to its maximum value.

The variations of vertical-velocity coefficient at maximum load and at exit are shown in figure 11 and the variations of time coefficient at maximum load, at maximum draft, and at exit are shown in figure 12. In general, the variations shown are pretty much of the type expected for a longitudinally straight model. However, the time of exit appears to show indications of bow effects at the low angles of trim where shorter times to exit are indicated than would be expected from the trends of the trims where the bow was not involved.

CONCLUDING REMARKS

An investigation to study the effects of transverse and longitudinal curvature on impact loads of chine-immersed models has been made in the Langley impact basin by use of a V-bottom model having a dead-rise angle of 30° and the forward half longitudinally curved upward on a radius of 10 beams. The impacts were made at fixed trim in smooth water over a range of trim angles of -3° to 30° and initial flight-path angles from 3.5° to 27° and a beam-loading coefficient of 18.8.

At maximum load the curved bow was largely immersed for 3° trim and below, only slightly immersed at 6° and 9° trim, and not immersed at 15° and 30° trim.

The maximum loads obtained with the curved-bow model vary less with trim angle than the loads predicted by theory for a straight-keel model. The experimental loads were less at low trims and greater at high trims than those predicted by theory for a straight-keel model.

The center of pressure at maximum impact load scattered about the value of 0.5 of the wetted length for the non-bow-immersed impacts and was in general greater than 0.6 for the bow-immersed impacts.

Maximum draft was independent of trim angle and apparently unaffected by bow immersion. However, the time to exit at low trim angles appeared to be less than would be expected from trends where the bow was not immersed.

Several general observations might be made in regard to the effects of bow curvature on impact loads of skis or seaplane hulls. First, at high angles of trim the curved bow would not be expected to enter into the impact process. This would indicate that impact loads on a ski or hull of the tested configuration (dead-rise angle of 30° and straight keel of 5 beams) and beam-loading coefficient (18.8) should be the same regardless of curved bow for given fixed-trim landings in the tested range of smooth-water operation (high trim and low flight-path angles). Loads for these landing conditions can be reasonably well predicted by the theory of NACA Report 1152. Second, the bow shape apparently does have an effect on impact loads of this model configuration landing on the sloping flank of a long wave (low trim and high flight-path angles relative to water surface). Indications are that the curved bow might result in reduced loads under these rough-water conditions. Prediction of loads by theory for these landing conditions has not been closely checked; therefore, the reduction due to bow curvature is only roughly indicated.

Langley Aeronautical Laboratory,
National Advisory Committee for Aeronautics,
Langley Field, Va., June 21, 1957.

REFERENCES

1. Edge, Philip M., Jr.: Impact-Loads Investigation of Chine-Immersed Models Having Concave-Convex Transverse Shape and Straight or Curved Keel Lines. NACA TN 3940, 1957.

2. Batterson, Sidney A.: The NACA Impact Basin and Water Landing Tests of a Float Model at Various Velocities and Weights. NACA Rep. 795, 1944. (Supersedes NACA WR L-163.)

3. Schnitzer, Emanuel: Theory and Procedure for Determining Loads and Motions in Chine-Immersed Hydrodynamic Impacts of Prismatic Bodies. NACA Rep. 1152, 1953. (Supersedes NACA TN 2813.)

4. Smiley, Robert F.: A Study of Water Pressure Distributions During Landings With Special Reference to a Prismatic Model Having a Heavy Beam Loading and a 30° Angle of Dead Rise. NACA TN 2111, 1950.

5. Batterson, Sidney A.: Variation of Hydrodynamic Impact Loads With Flight-Path Angle for a Prismatic Float at 0° and -3° Trim and With a $22\frac{1}{2}^{\circ}$ Angle of Dead Rise. NACA TN 1166, 1947.

TABLE I.- IMPACT-LOADS DATA FROM TESTS OF A MODEL WITH 30° DEAD-RISE ANGLE AND CURVED BOW

Run	At contact				At $n_{1,max}$									At z_{max}		At exit	
	$\dot{x}_o$, ft/sec	$\dot{z}_o$, ft/sec	V_o, ft/sec	γ_o, deg	t, sec	z, ft	$\dot{z}$, ft/sec	n_1	l_w, ft	M_Y, ft-lb	C_L	C_m	C_p	t, sec	z, ft	t, sec	$\dot{z}$, ft/sec
$\tau = -3^\circ$																	
1	73.0	4.8	73.2	4.04	0.170	0.65	2.0	0.8	8.97	8,645	0.2	1.7	8.3	0.245	0.71	-----	----
2	71.4	8.0	71.9	6.50	.136	.84	3.1	1.2	9.43	12,934	.3	2.6	9.1	.217	.96	0.764	-1.6
3	65.4	11.8	66.4	10.23	.046	.50	10.0	1.9	9.34	13,555	.5	3.2	6.0	.246	1.39	.685	-2.6
4	65.8	12.1	66.9	10.46	.050	.54	9.9	2.0	9.46	14,811	.5	3.4	6.3	.240	1.36	.709	-2.4
5	48.8	11.8	50.2	13.54	.046	.51	9.7	1.9	9.40	12,553	.9	5.1	5.6	.301	1.54	.852	-2.2
$\tau = 0^\circ$																	
6	87.0	5.4	87.1	3.53	0.055	0.25	4.4	0.7	7.32	5,283	0.1	0.7	6.0	0.238	0.66	-----	----
7	78.1	9.1	78.7	6.61	.039	.33	7.5	1.7	7.67	10,378	.3	1.7	5.2	.196	.86	0.448	-2.3
8	66.2	11.8	67.3	10.06	.033	.38	9.8	2.3	7.82	13,419	.6	3.1	5.0	.222	1.22	.628	-3.1
9	41.8	11.0	43.3	14.78	.034	.35	9.4	1.9	7.69	10,848	1.3	6.0	4.7	.311	1.46	1.018	-1.5
10	32.3	12.1	34.5	20.56	.031	.36	10.0	2.1	7.72	10,678	2.1	9.3	4.3	.365	1.74	1.251	-1.3
11	0	4.7	4.7	90.00	.058	.25	4.1	.4	7.42	1,805	---	---	3.6	.514	1.26	-----	----
12	0	5.5	5.5	90.00	.058	.30	4.8	.5	7.58	2,139	---	---	3.5	.517	1.46	-----	----
13	0	6.1	6.1	90.00	.049	.28	5.3	.7	7.27	2,964	---	---	3.7	.516	1.54	-----	----
14	0	7.2	7.2	90.00	.048	.31	6.0	.8	7.56	3,427	---	---	3.7	.507	1.70	-----	----
15	0	7.4	7.4	90.00	.044	.30	6.5	.9	7.50	4,044	---	---	3.8	.510	1.77	-----	----
16	0	8.6	8.6	90.00	.033	.26	7.4	1.0	7.13	4,075	---	---	3.5	.526	2.01	-----	----
17	0	10.2	10.2	90.00	.031	.30	8.9	1.4	7.50	6,317	---	---	3.7	.539	2.33	-----	----
18	0	12.4	12.4	90.00	.022	.36	10.6	1.9	7.64	8,141	---	---	3.6	.568	2.68	-----	----
$\tau = 3^\circ$																	
19	88.5	5.5	88.7	3.53	0.100	0.45	3.4	0.9	6.40	3,657	0.1	0.5	3.6	0.265	0.71	-----	----
20	78.7	9.4	79.3	6.82	.066	.57	6.4	1.9	6.98	9,137	.4	1.5	4.0	.210	1.02	0.702	-1.7
21	65.8	12.2	66.9	10.53	.056	.61	8.8	2.5	7.15	13,646	.7	3.1	4.7	.237	1.24	.729	-2.3
22	46.5	12.1	46.3	14.58	.054	.58	9.4	2.1	6.98	11,682	1.1	5.2	4.6	.295	1.54	1.094	-1.1
23	31.9	12.4	33.7	21.29	.049	.55	10.1	1.8	6.75	9,651	1.9	8.5	4.5	.373	1.88	1.483	-4.2
$\tau = 6^\circ$																	
24	88.5	5.6	88.7	3.61	0.131	0.57	3.3	1.2	4.98	3,328	0.2	0.4	2.4	0.201	0.69	0.571	-1.6
25	78.7	10.9	79.5	7.89	.067	.60	6.6	2.3	5.45	8,821	.4	1.4	3.1	.195	.98	.565	-3.2
26	67.1	12.1	67.1	10.25	.063	.69	8.1	2.6	5.72	8,584	.7	1.9	2.8	.232	1.26	.705	-3.0
27	66.7	12.1	66.7	10.29	.068	.72	8.2	2.4	6.01	7,904	.6	1.8	2.8	.232	1.29	.720	-2.9
28	67.6	12.3	67.6	10.30	.068	.73	8.4	2.5	6.01	7,780	.6	1.7	2.6	.231	1.28	.707	-3.0
29	65.8	12.0	65.8	10.31	.069	.73	7.9	2.4	6.01	8,588	.6	2.0	3.0	.240	1.29	.769	-2.4
30	46.3	12.5	48.0	15.11	.068	.76	9.2	2.0	6.21	6,979	1.1	3.1	2.9	.293	1.59	.993	-2.1
31	41.8	12.5	43.7	16.68	.071	.68	9.1	1.9	5.96	6,075	1.2	3.3	2.7	.314	1.71	1.094	-1.9
32	32.2	12.3	34.5	20.92	.067	.77	9.2	1.6	6.30	5,580	1.6	4.8	2.9	.369	1.92	1.289	-1.3
33	22.5	11.0	25.0	26.17	.065	.69	9.0	1.3	5.86	4,154	2.5	6.8	2.7	.460	2.10	1.322	-2.0
$\tau = 9^\circ$																	
34	89.3	5.6	88.1	3.58	0.099	0.46	2.8	1.3	2.85	1,866	0.2	0.2	1.2	0.173	0.54	0.410	-2.9
35	79.4	9.6	78.7	6.89	.089	.65	5.3	2.1	4.22	6,271	.4	1.0	2.5	.184	.94	.495	-4.1
36	66.9	12.0	66.9	10.18	.088	.86	7.0	2.4	5.45	9,481	.6	2.1	3.3	.221	1.26	.707	-3.1
37	46.7	12.6	47.6	15.10	.080	.89	8.7	1.9	5.48	6,401	1.0	2.8	2.9	.287	1.62	.903	-3.1
38	33.1	12.2	35.3	20.27	.086	.97	8.6	1.7	6.07	6,579	1.6	5.5	3.3	.374	1.97	1.224	-2.0
39	23.9	12.2	26.9	27.08	.077	.87	9.4	1.4	5.50	4,821	2.4	6.9	2.8	.352	2.65	1.320	-2.6
$\tau = 15^\circ$																	
40	83.3	5.5	82.2	3.78	0.110	0.47	2.0	1.4	1.82	1,240	0.7	0.2	0.7	0.156	0.51	0.359	-3.3
41	74.1	8.5	73.4	6.58	.097	.71	4.4	1.8	2.73	2,666	.4	.5	1.2	.180	.88	.436	-4.6
42	66.7	12.1	66.7	10.29	.090	.91	6.3	2.5	3.52	6,027	.7	1.4	2.0	.185	1.23	.495	-5.4
43	45.5	12.1	47.0	14.91	.097	.99	7.5	1.8	3.82	4,955	1.0	2.3	2.3	.265	1.58	.785	-3.7
44	26.6	12.2	28.8	24.69	.095	.95	9.0	1.3	3.67	4,227	1.8	5.1	2.7	.425	2.21	1.483	-1.6
$\tau = 30^\circ$																	
45	78.1	9.6	77.5	7.00	0.101	0.73	3.0	3.0	1.45	2,815	0.6	0.5	0.7	0.142	0.79	0.299	-7.7
46	68.0	11.8	68.0	9.87	.097	.94	5.9	2.7	1.88	2,804	.7	.6	.8	.169	1.16	.383	-8.0
47	45.9	12.4	46.8	15.14	.164	1.41	5.5	1.8	2.82	2,832	1.0	1.3	1.1	.237	1.53	.578	-6.3
48	32.3	12.1	33.9	20.50	.165	1.57	5.7	1.4	3.14	2,989	1.4	2.6	1.6	.312	1.99	.880	-4.6
49	23.6	10.9	26.0	24.83	.176	1.64	6.7	1.0	3.28	2,505	1.8	3.8	1.9	.460	2.47	1.454	-2.2

TABLE II.- DRAFT AT BEGINNING OF CURVATURE IMMERSION FOR A MODEL WITH 30° DEAD-RISE ANGLE AND CURVED BOW

τ, deg	z_k, ft (a)	z_c, ft (b)
-3	0	0.29
0	0	.29
3	.26	.55
6	.53	.81
9	.79	1.1
15	1.3	1.6
30	2.5	2.8

[a]Draft at keel curvature immersion.

[b]Draft at chine curvature immersion.

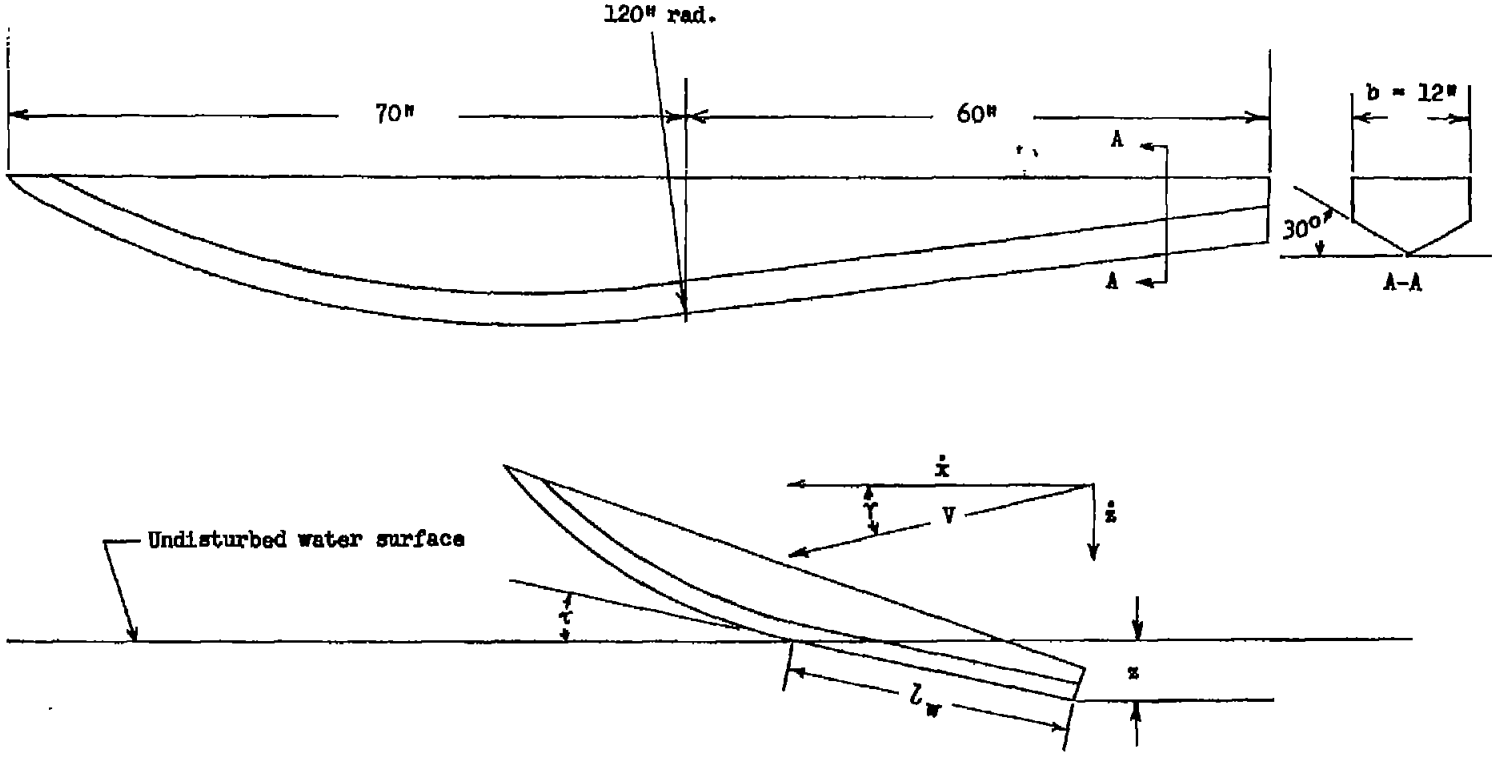

Figure 1.- Profile showing pertinent dimensions of model with 30° dead-rise angle and curved bow tested in Langley impact basin and the geometric relations during impact.

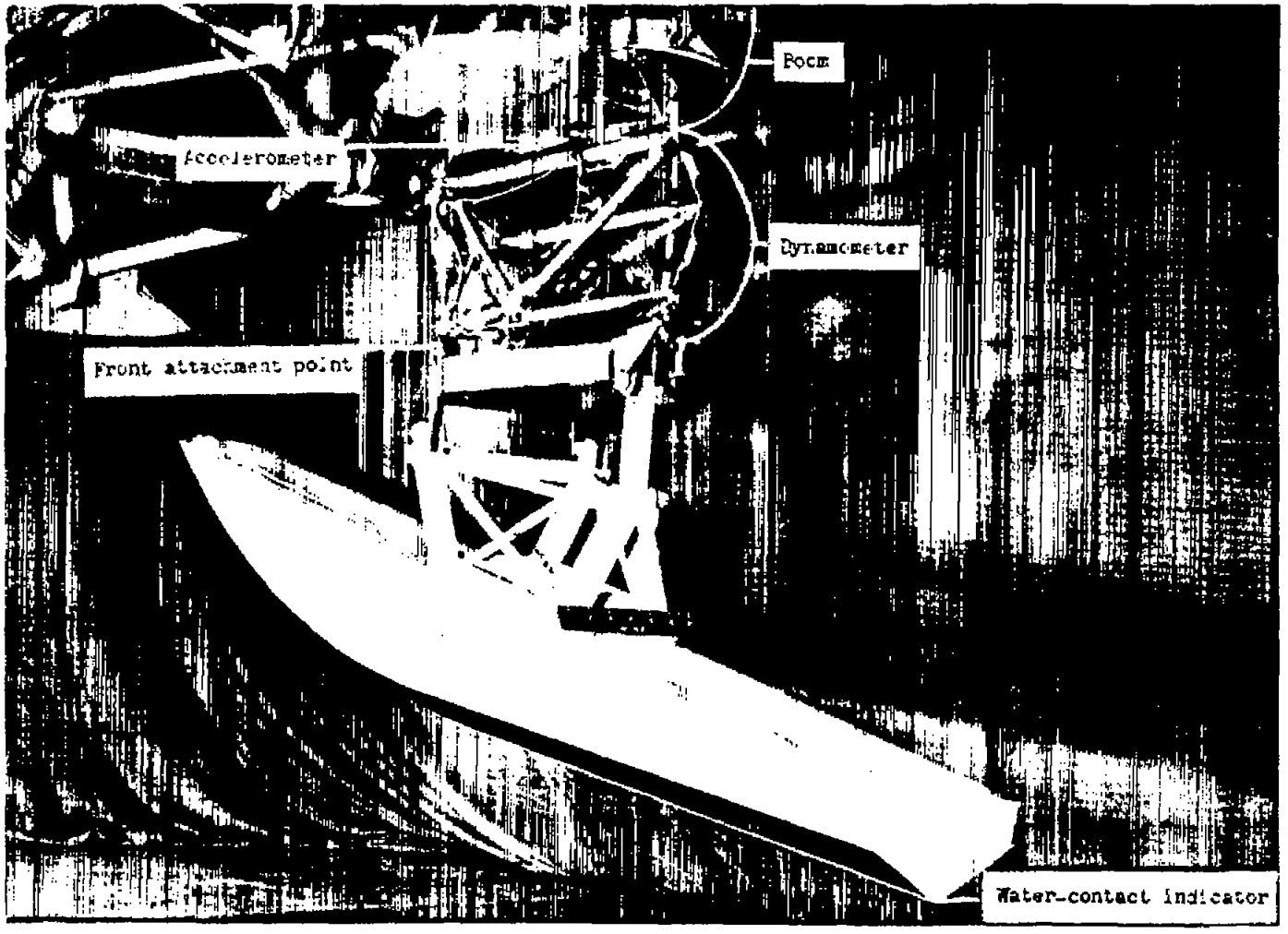

L-92759.1

Figure 2.- Photograph of model with 30° dead-rise angle and curved bow attached to impact-basin carriage.

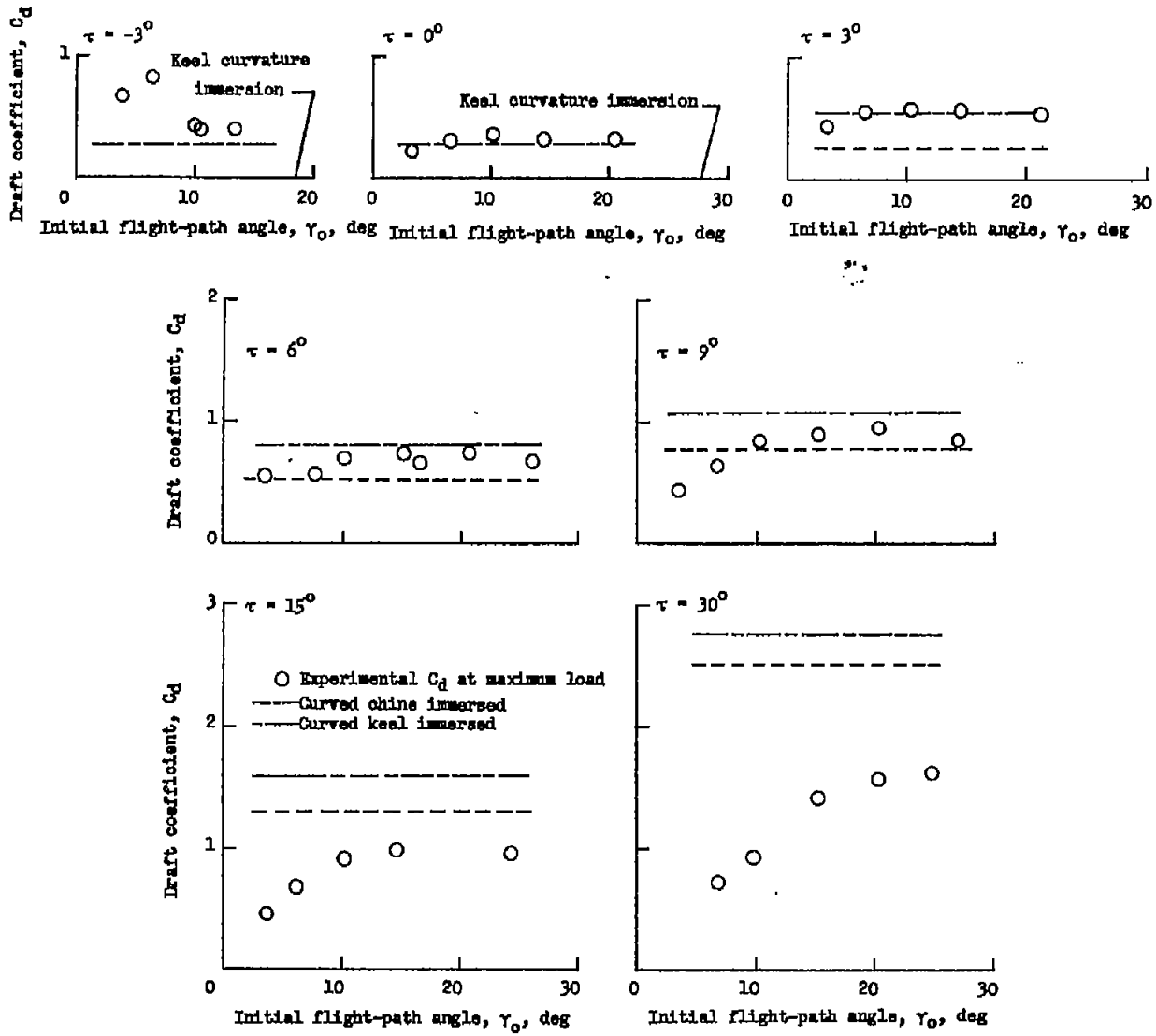

Figure 3.- Experimental variation of draft at maximum impact load with initial flight-path angle.

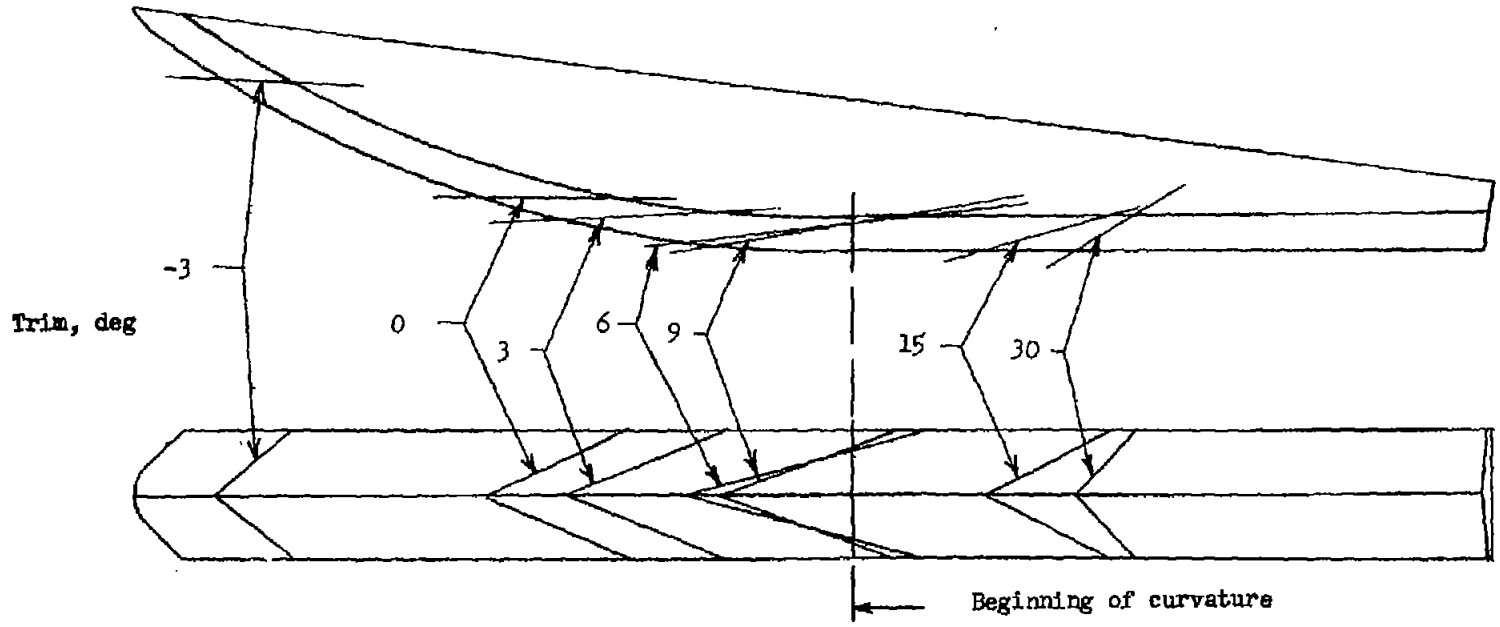

Figure 4.- Intersection of model and undisturbed water surface for maximum immersion at maximum impact load for each trim angle.

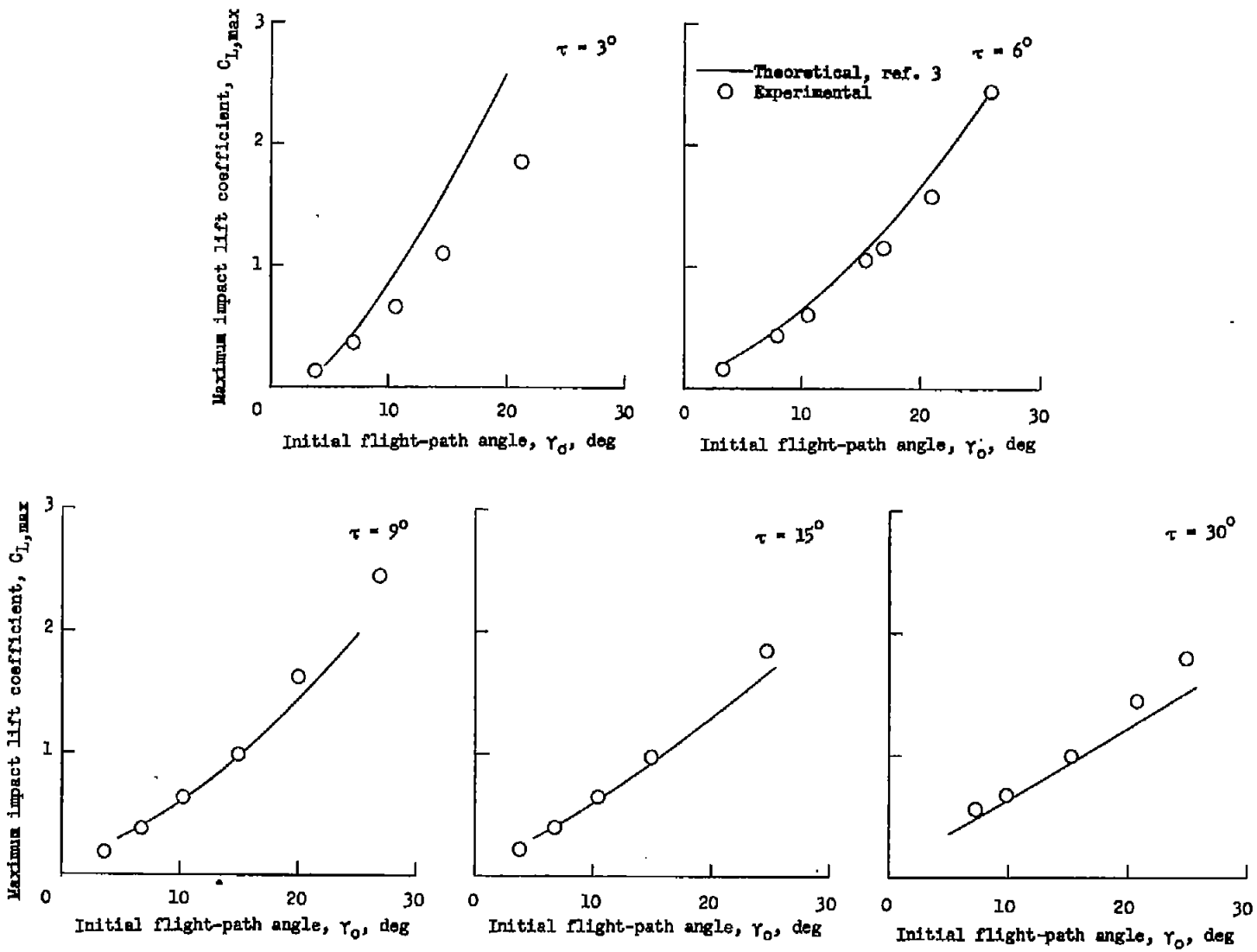

Figure 5.- Comparison of theoretical and experimental maximum impact lift coefficients.

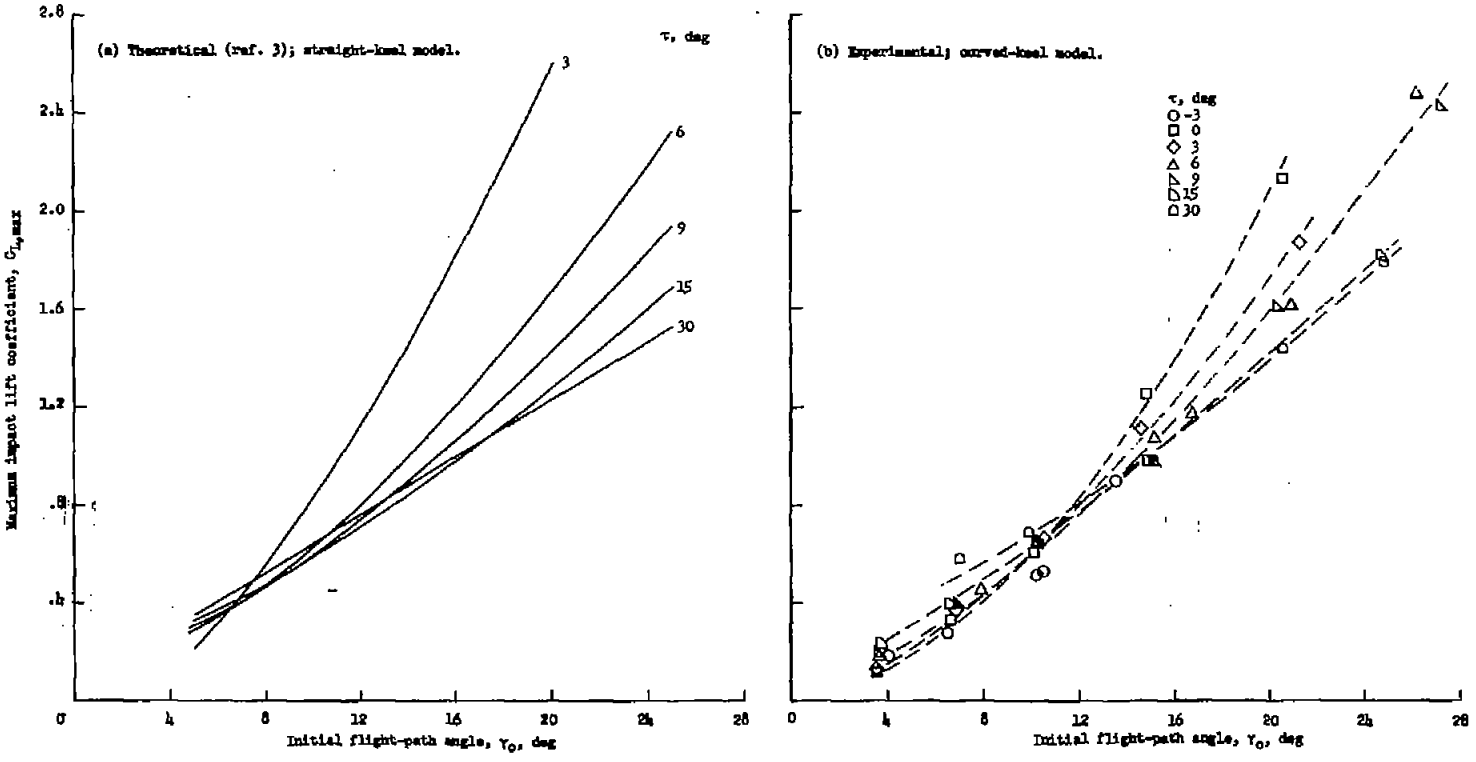

Figure 6.- Comparison of theoretical and experimental trends of maximum impact lift coefficients.

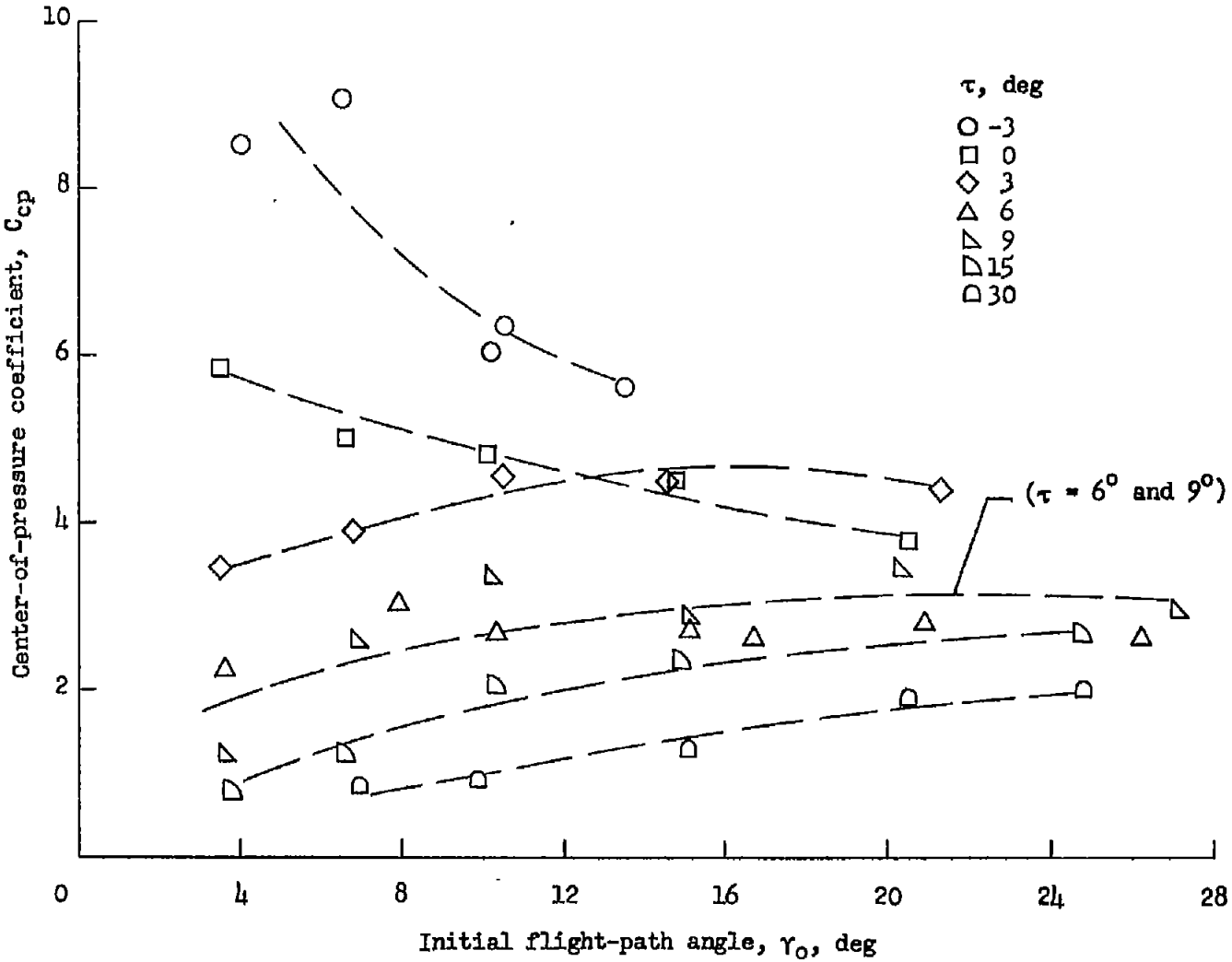

Figure 7.- Experimental variation of center-of-pressure coefficient at maximum impact load with initial flight-path angle and trim angle.

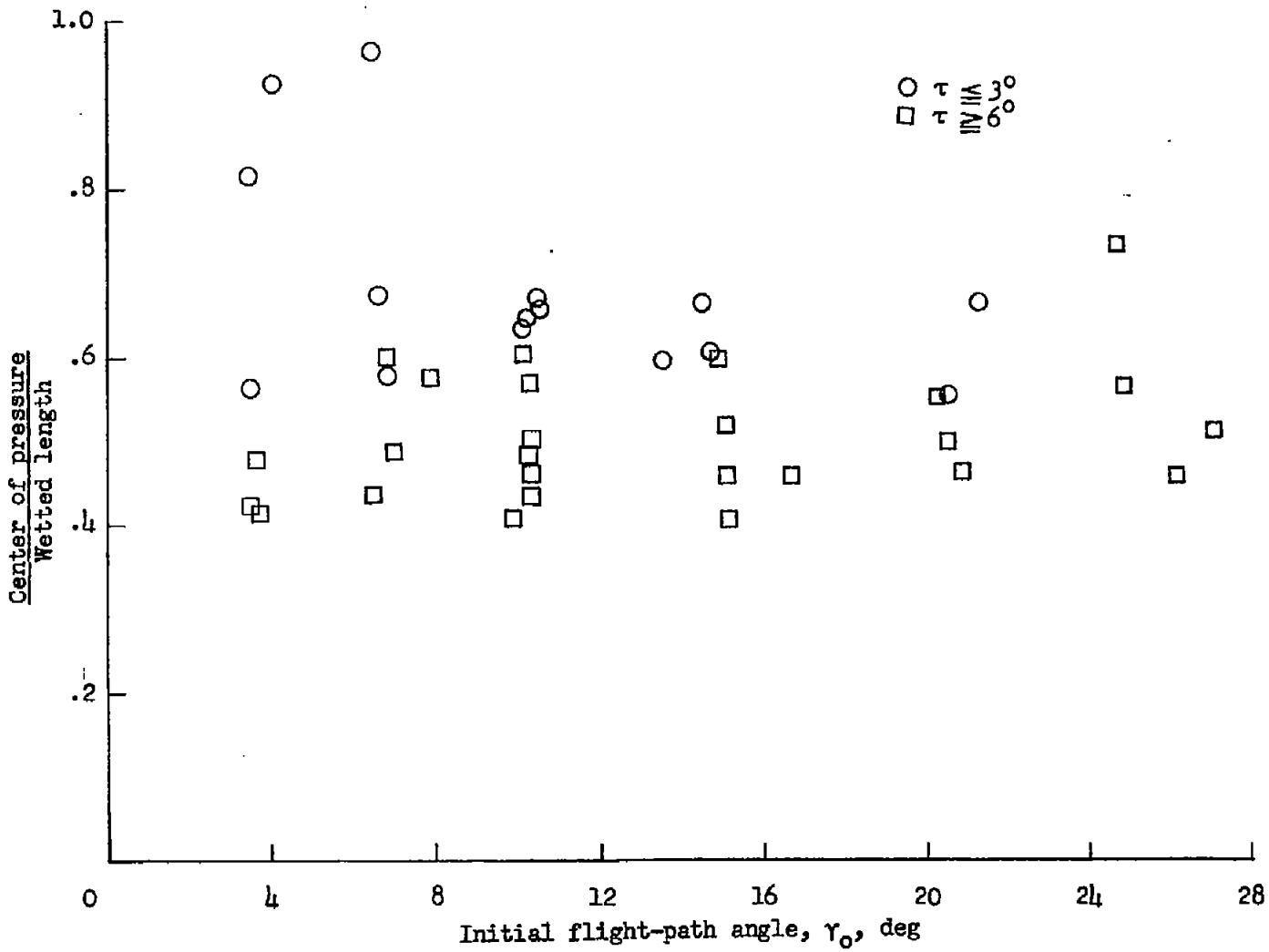

Figure 8.- Experimental variation with initial flight-path angle of ratio of center-of-pressure distance to wetted length, at maximum impact load.

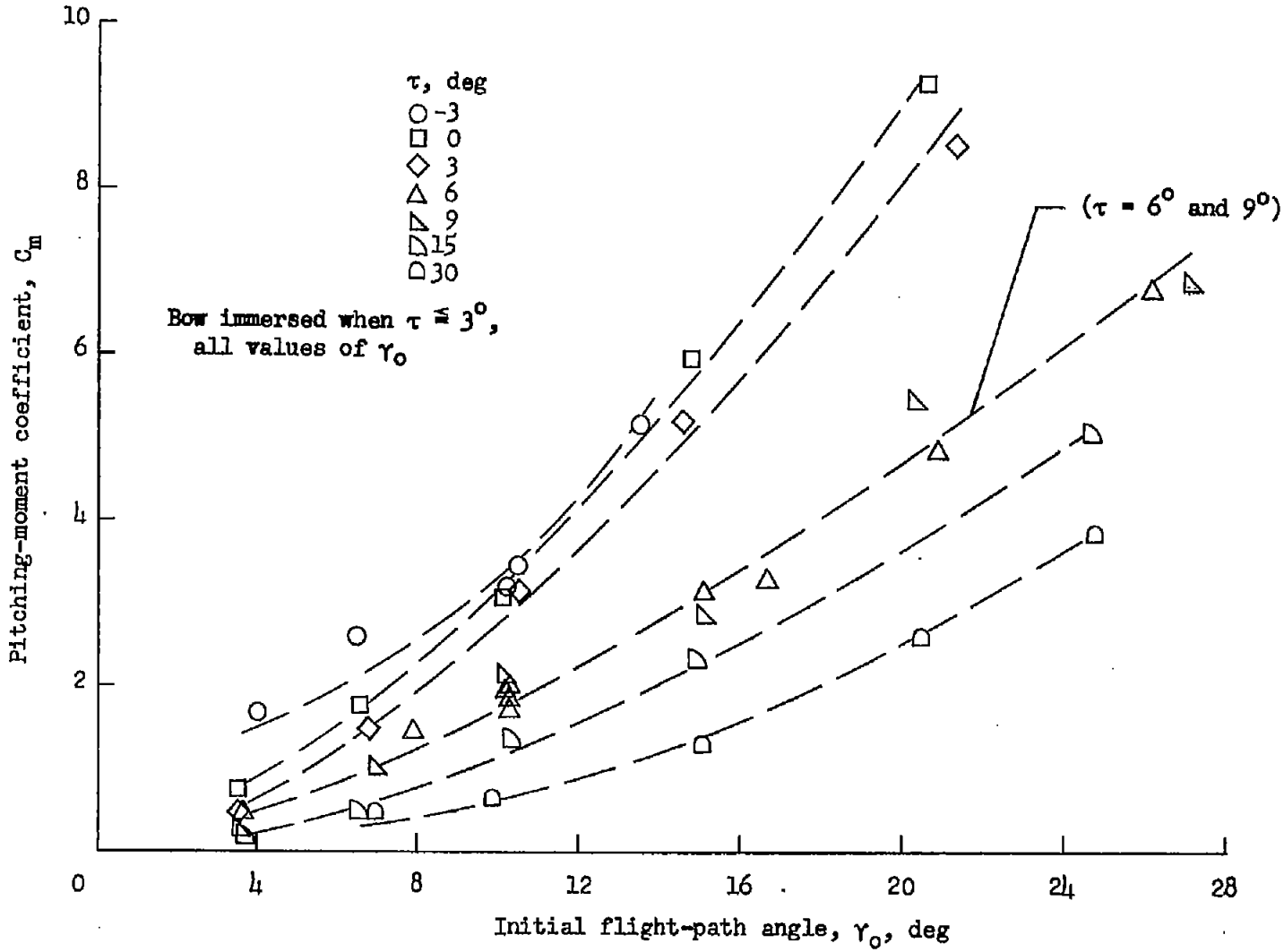

Figure 9.- Experimental variation of pitching-moment coefficient at maximum impact load with initial flight-path angle and trim angle.

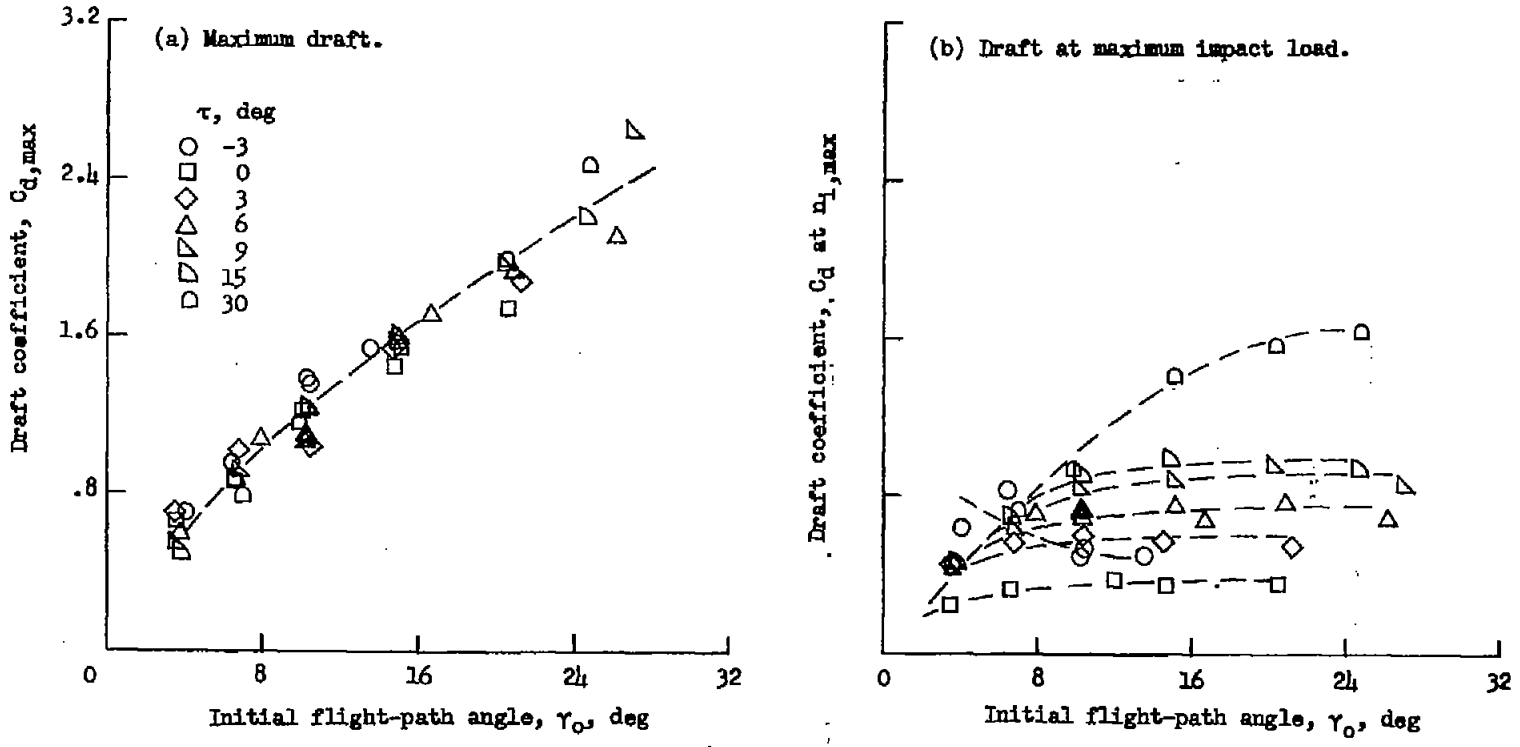

Figure 10.- Experimental variations of maximum draft and draft at maximum impact load with initial flight-path angle and trim angle.

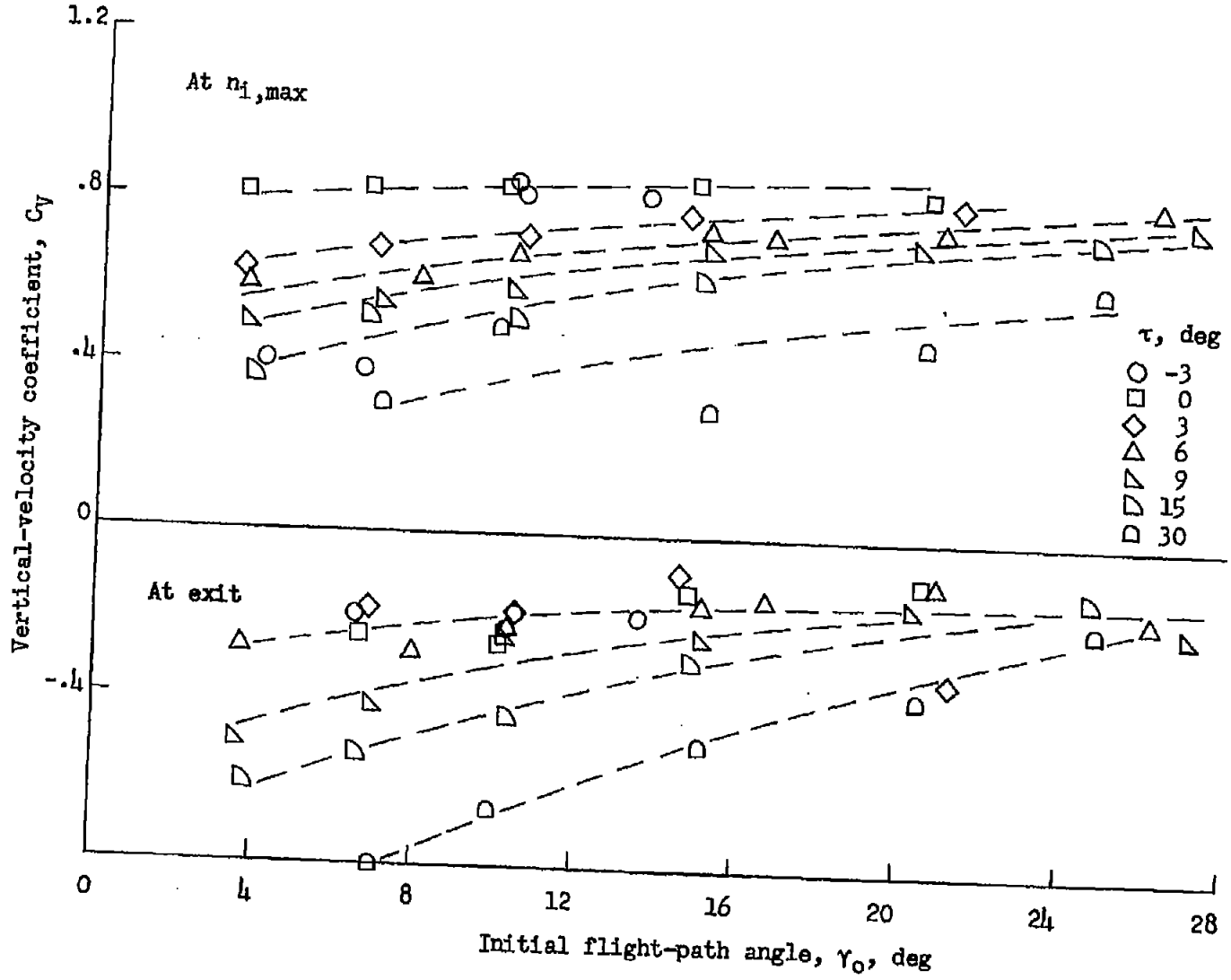

Figure 11.- Experimental variation of vertical-velocity coefficient at maximum impact load and at exit with initial flight-path angle and trim angle.

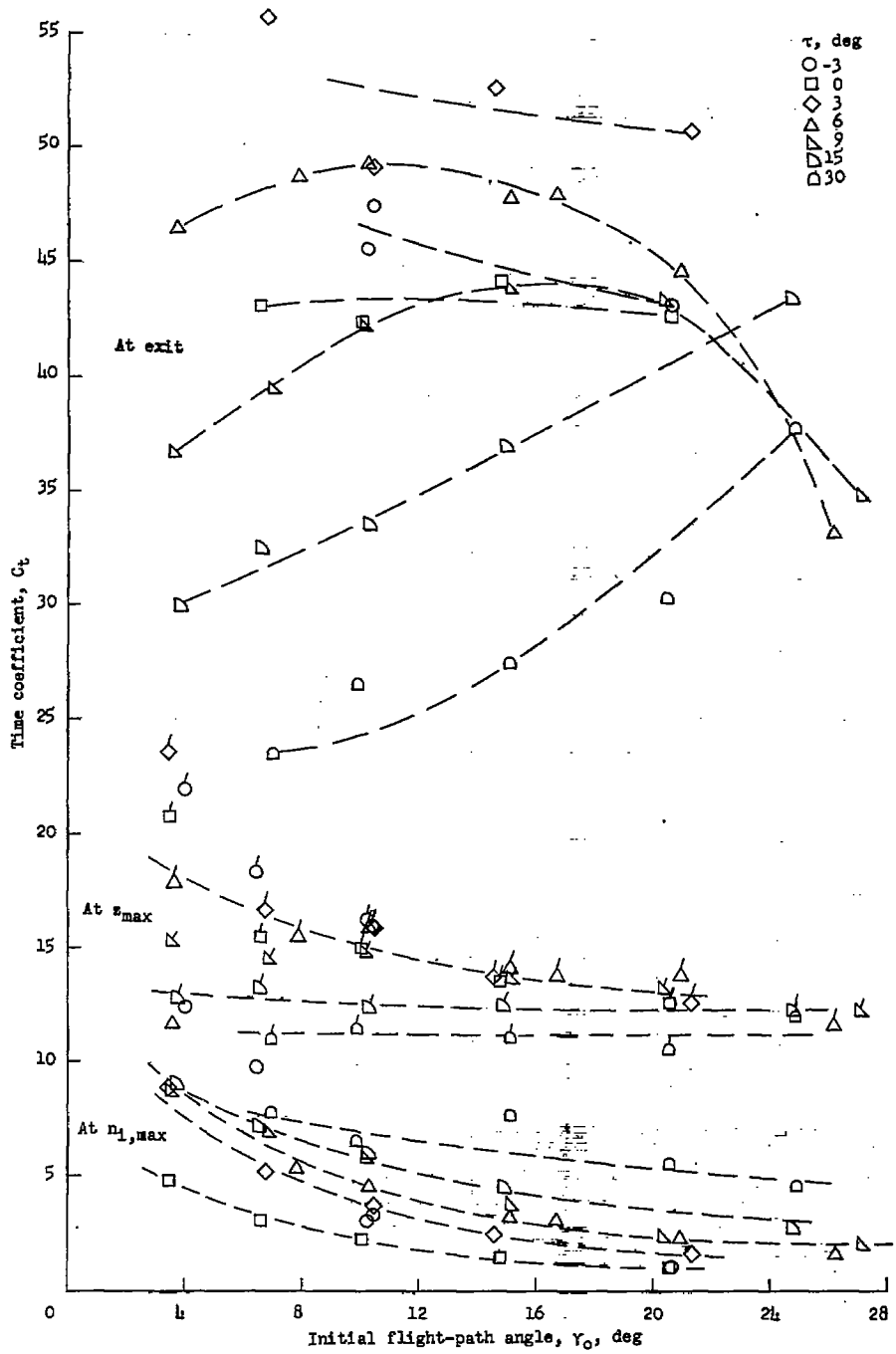

Figure 12.- Experimental variation of time coefficient at maximum impact load, maximum draft, and exit with initial flight-path angle and trim angle. Flagged symbols denote C_t at z_{max}.